A Theoretical Investigation of 2D MAXY-*J*RES NMR Spectroscopy of CD_nCD_m Groups

İrfan Şaka and Azmi Gençten

Department of Physics, Faculty of Arts and Sciences, Ondokuz Mayıs University, 55139, Samsun, Turkey

Reprint requests to A. G.; Fax: +90 362 4576081; E-mail: gencten@omu.edu.tr

Z. Naturforsch. **63a,** 339 – 350 (2008); received September 4, 2007

There exists a variety of multiple-pulse NMR experiments for spectral editing of complex molecules in solution. Maximum quantum correlation NMR (MAXY NMR) spectroscopy is one of the techniques for distinguishing CH_n groups by editing ^1H NMR spectra. Spectral assignments of 2D homonuclear *J*-resolved NMR spectroscopy become too difficult, due to complex overlapping spectra. In order to overcome this problem a new technique called 2D MAXY-*J*RES NMR spectroscopy, which is the combination of MAXY NMR and homonuclear *J*-resolved NMR spectroscopy, is used. In this study, product operator description of 2D MAXY-*J*RES NMR spectroscopy is performed for $IS_nI'S'_m$ ($I = I' = \frac{1}{2}$; $S = S' = 1$; $n = 1,2,3$; $m = 1,2$) multi-spin systems. Experimental suggestions are made and simulated spectra are presented for the 2D MAXY-*J*RES NMR experiment. Therefore, it is shown that 2D MAXY-*J*RES NMR spectroscopy can be used to distinguish CD, CD_2 and CD_3 groups from each other in CD_nCD_m groups.

Key words: NMR; MAXY-*J*RES; Product Operator Formalism; Spin-1.

1. Introduction

There exists a large number of homo- and heteronuclear multiple-pulse 1D, 2D and 3D nuclear magnetic resonance (NMR) experiments. Maximum quantum correlation (MAXY) NMR spectroscopy is one of the techniques for distinguishing CH_n groups by editing ^1H NMR spectra [1 – 7]. ^{13}C NMR spectroscopy is also widely used in editing methods such as DEPT [8] and SEMUT [9]. Editing and selective detection methods for ^1H NMR spectroscopy are reviewed in [10]. In homonuclear *J*-resolved NMR spectroscopy, the chemical shift and spin-spin coupling parameters are resolved along the two different axes for the same kind of coupled nuclei such as ^1H. Sometimes, spectral assignments of 2D homonuclear *J*-resolved NMR spectroscopy become too difficult, due to complex overlapping spectra. In order to overcome this problem a new technique called 2D MAXY-*J*RES NMR spectroscopy, which is the combination of MAXY and homonuclear *J*-resolved NMR spectroscopy, is used [3]. This technique is used to distinguish CH_nCH_m groups in complex samples such as biological fluids [3]. ^2H NMR spectroscopy became a powerful technique for different applications such as deuterium labelling and structure elucidation [11]. Therefore, 2D MAXY-*J*RES NMR spectroscopy can be also used for the identification of CD_nCD_m groups in complex samples.

As NMR is a quantum mechanical phenomenon, nuclear spin systems can be treated by quantum mechanical methods. The product operator formalism, as a simple quantum mechanical method, has been developed for the analytical description of multiple-pulse NMR experiments of weakly coupled spin systems in liquids having spin-1/2 and spin-1 nuclei [12 – 22]. In this formalism, the spin operators themselves and their direct products, called product operators, are used. By using the product operator theory, SEMUT NMR spectroscopy is applied to CD_n groups [23]. Experimental and theoretical investigations of ^{13}C DEPT NMR spectroscopy of CD_n systems are presented in [24]. For CH_n and CD_n groups, the product operator theory of a 2D DEPT *J*-resolved NMR experiment is investigated [25, 26]. Product operator descriptions of MAXY and MAXY-HMQC NMR experiments of CD_n groups are also reported in our recent studies [27, 28]. The product operator theory for spin-3/2 and its application to 2D *J*-resolved NMR spectroscopy is reported [29]. For spin systems having spin-3/2 nuclei,

0932–0784 / 08 / 0500–0339 $ 06.00

by using the product operator formalism, theoretical investigations of 3D *J*-resolved, DEPT, SEMUT, INEPT and RINEPT NMR experiments are also presented [30 – 32]. The product operator theory of high resolution solution state double quantum spectroscopy of two spin-1 AX systems are investigated [21, 33, 34]. By using the product operator theory in NMR experiments, experimental results can be confirmed and also new experimental suggestions can be made [19, 23]. In the present study experimental suggestions are made.

In the present study, first, evolutions of some product operators under the homonuclear scalar spin-spin coupling Hamiltonian for a SS' ($S = 1$, $S' = 1$) spin system are obtained. Then, by using the product operator formalism, theoretical results are obtained for the 2D MAXY-*J*RES NMR experiment of $IS_nI'S'_m$ ($I = I' = 1/2$; $S = S' = 1$; $n = 1,2,3$; $m = 1,2$) multispin systems. By using the obtained theoretical results, experimental suggestions are presented, and simulated spectra of various groups are obtained for the 2D MAXY-*J*RES NMR experiment. To the best of our knowledge, this will be the first product operator description of a 2D MAXY-*J*RES NMR experiment of CD$_n$CD$_m$ groups. As a result, it is shown that one can perform this experiment to distinguish CD, CD$_2$ and CD$_3$ groups in CD$_n$CD$_m$ systems.

2. Theory

The product operator theory is the expansion of the density matrix operator in terms of matrix representation of angular momentum operators for individual spins. For the IS ($I = 1/2$, $S = 1$) spin system, four Cartesian spin angular momentum operators for $I = 1/2$, E_I, I_x, I_y, I_z, and nine Cartesian spin angular momentum operators for $S = 1$, E_S, S_x, S_y, S_z, S_z^2, $[S_x,S_z]_+$, $[S_y,S_z]_+$, $[S_x,S_y]_+$, $(S_x^2 - S_y^2)$, can be easily found [35]. So, $4 \times 9 = 36$ product operators for the IS ($I = 1/2$, $S = 1$) spin system are obtained with direct products of these angular momentum operators. For the IS ($I = 1$, $S = 1$) spin system there will be $9 \times 9 = 81$ product operators.

Time dependence of the density matrix is governed by the Liouville-von Neumann equation:

$$\frac{\mathrm{d}\sigma}{\mathrm{d}t} = \frac{\mathrm{i}}{\hbar}[\sigma,\mathcal{H}], \tag{1}$$

where $[\sigma,\mathcal{H}]$ is the commutator of the density matrix, σ, and the Hamiltonian, $\mathcal{H}$. When the Hamiltonian is time-independent, the solution of the (1) is

$$\sigma(t) = \exp(-\mathrm{i}\mathcal{H}t)\sigma(0)\exp(\mathrm{i}\mathcal{H}t), \tag{2}$$

where $\mathcal{H}$ is the total Hamiltonian which consists of radiofrequency (r. f.) pulse, chemical shift and spin-spin coupling Hamiltonians, and $\sigma(0)$ is the density matrix at $t = 0$. After employing the Hausdorff formula [16]

$$\begin{aligned}\exp(-\mathrm{i}\mathcal{H}t)A\exp(\mathrm{i}\mathcal{H}t) &= A - (\mathrm{i}t)[\mathcal{H},A]\\ &+ \frac{(\mathrm{i}t)^2}{2!}[\mathcal{H},[\mathcal{H},A]] - \frac{(\mathrm{i}t)^3}{3!}[\mathcal{H},[\mathcal{H},[\mathcal{H},A]]] + \cdots,\end{aligned} \tag{3}$$

evolutions of product operators under the r. f. pulse, chemical shift and spin-spin coupling Hamiltonians can be easily obtained [12, 16, 18]. A complete product operator theory for the IS ($I = 1/2$, $S = 1$) spin system and its application to the DEPT-HMQC NMR experiment is presented in our recent study [36]. For the IS ($I = 1$, $S = 1$) spin system the evolutions of some product operators under the spin-spin coupling Hamiltonian ($\mathcal{H}_J = 2\pi J I_z S_z$) are known; they are given as follows [21, 33, 34]:

$$\begin{aligned}I_xS_y \xrightarrow{\mathcal{H}_Jt} &\frac{1}{2}I_xS_y(c_{2J}+1) + \frac{1}{2}I_{yz}S_{xz}(c_{2J}-1)\\ &+ \frac{1}{2}(I_yS_{yz} - I_{xz}S_x)s_{2J},\end{aligned} \tag{4}$$

$$\begin{aligned}I_zS_x^2 \xrightarrow{\mathcal{H}_Jt} &\frac{1}{2}I_zS_x^2(c_{4J}+1) - \frac{1}{2}I_zS_y^2(c_{4J}-1)\\ &+ \frac{1}{2}I_z^2S_{xy}s_{4J},\end{aligned} \tag{5}$$

$$\begin{aligned}I_zS_y^2 \xrightarrow{\mathcal{H}_Jt} &\frac{1}{2}I_zS_y^2(c_{4J}+1) - \frac{1}{2}I_zS_x^2(c_{4J}-1)\\ &- \frac{1}{2}I_z^2S_{xy}s_{4J}.\end{aligned} \tag{6}$$

In these equations, $I_{yz} = [I_y,I_z]_+$, $I_{xz} = [I_x,I_z]_+$, $S_{xz} = [S_x,S_z]_+$, $S_{yz} = [S_y,S_z]_+$, and $S_{xy} = [S_x,S_y]_+$. For this spin system the evolutions of some other product operators under the spin-spin coupling Hamiltonian are obtained and presented in the following section. At any time during the experiment, the ensemble averaged expectation value of the spin angular momentum, e. g. for I_y, is

$$\langle I_y\rangle = \mathrm{Tr}[I_y\sigma(t)], \tag{7}$$

where $\sigma(t)$ is the density matrix operator calculated from (2) at any time. As $\langle I_y\rangle$ is proportional to the magnitude of the y-magnetization, it represents the signal

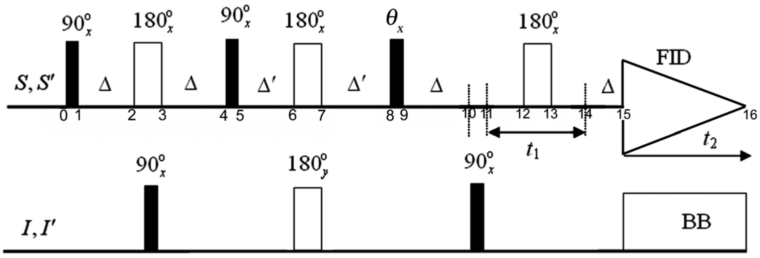

Fig. 1. Pulse sequence of the 2D MAXY-*J*RES NMR experiment [3].

detected on the *y*-axis. So, in order to estimate the free induction decay (FID) signal of a multiple-pulse NMR experiment, the density matrix operator should be obtained at the end of the experiment.

3. Evolutions of Some Product Operators under the Spin-Spin Coupling Hamiltonian

As the homonuclear spin-spin coupling occurs between two spin-1 nuclei (S and S' spin) during t_1 in the 2D MAXY-*J*RES NMR experiment, we need to obtain the evolutions of some product operators under the homonuclear scalar spin-spin coupling Hamiltonian, $\mathcal{H}(S-S') = 2\pi J_{SS'}S_zS'_z$. By using the Hausdorff formula, evolution of the S_x^2 product operator under the spin-spin coupling Hamiltonian can be obtained as

$$\begin{aligned} S_x^2 \xrightarrow{\mathcal{H}_{SS'}t} & \exp(-2i\pi JS_zS'_zt)S_x^2\exp(2i\pi JS_zS'_zt) \\ &= S_x^2 - (i2\pi Jt)A(1) + \frac{(i2\pi Jt)^2}{2!}A(2) \\ &- \frac{(i2\pi Jt)^3}{3!}A(3) + \ldots, \end{aligned} \tag{8}$$

$$A(1) = [S_zS'_z, S_x^2], \tag{9}$$

$$A(2) = [S_zS'_z, A(1)], \tag{10}$$

$$A(3) = [S_zS'_z, A(2)]. \tag{11}$$

Using commutation relations and $S_i^n \equiv S_i^{n-2}$ ($n \geq 3$) for spin-1,

$$\begin{aligned} S_x^2 \xrightarrow{\mathcal{H}_{SS'}t} S_x^2 &- \frac{1}{2}\left\{\frac{(4\pi Jt)^2}{2!}(S_x^2 - S_y^2)S_z'^2 + \ldots\right\} \\ &+ \frac{1}{2}\left\{(4\pi Jt)[S_x,S_y]_+S'_z\right. \\ &\left. - \frac{(4\pi Jt)^3}{3!}[S_x,S_y]_+S'_z + \ldots\right\} \end{aligned} \tag{12}$$

is obtained. In order to get the generalized form for the evolution of the S_x^2 product operator under the spin-spin coupling Hamiltonian, some additions and subtractions can be made; then one obtains the following shorthand notation form:

$$S_x^2 \xrightarrow{2\pi JS_zS'_zt} S_x^2 + \frac{1}{2}(S_x^2 - S_y^2)S_z'^2(c_{4J} - 1) + \frac{1}{2}S_{xy}Sz's_{4J}. \tag{13}$$

Here, and in the following equations, $S_{xz} = [S_x,S_z]_+$, $S_{yz} = [S_y,S_z]_+$, $S_{xy} = [S_x,S_y]_+$, $c_{nJ} = \cos(n\pi Jt_1)$ and $s_{nJ} = \sin(n\pi Jt_1)$. For the remaining product operators, the similar procedure is applied and the obtained results are given in Table 1. Similar evolutions can be easily obtained for the product operators $S_x'^2$, $S_y'^2$, S'_{xz}, S'_{yz}, and S'_{xy} under the scalar spin-spin coupling Hamiltonian.

Table 1. Evolutions of some product operators under the spin-spin coupling Hamiltonian ($\mathcal{H}_{SS'} = 2\pi J_{SS'}S_zS'_z$). $S_{xz} = [S_x,S_z]_+$, $S_{yz} = [S_y,S_z]_+$, and $S_{xy} = [S_x,S_y]_+$.

Product operator	Evolution of product operator under the spin-spin coupling Hamiltonian
S_x^2	$S_x^2 + \frac{1}{2}(S_x^2 - S_y^2)S_z'^2(c_{4J} - 1) + \frac{1}{2}S_{xy}S'_zs_{4J}$
S_y^2	$S_y^2 - \frac{1}{2}(S_x^2 - S_y^2)S_z'^2(c_{4J} - 1) - \frac{1}{2}S_{xy}S'_zs_{4J}$
S_{xz}	$S_{xz} + S_{xz}S_z'^2(c_{2J} - 1) + S_{yz}S'_zs_{2J}$
S_{yz}	$S_{yz} + S_{yz}S_z'^2(c_{2J} - 1) - S_{xz}S'_zs_{2J}$
S_{xy}	$S_{xy} + S_{xy}S_z'^2(c_{4J} + 1) - (S_x^2 - S_y^2)S'_zs_{4J}$

4. Results and Discussion

In this section, the analytical descriptions of 2D MAXY-*J*RES NMR spectroscopy of $IS_nI'S'_m$ ($I = I' = \frac{1}{2}$; $S = S' = 1$; $n = 1,2,3$; $m = 1,2$) multi-spin systems are presented by using the product operator theory. This section is divided into two subsections. In the first one, theoretical results for the analytical description of the 2D MAXY-*J*RES experiment are obtained; in the second one, experimental suggestions and simulated spectra for several CD_nCD_m groups are presented.

4.1. Product Operator Theory

For the product operator description of the 2D MAXY-*J*RES NMR experiment, the pulse sequence,

Table 2. Evolutions of nine angular momentum operators under the r. f. pulse Hamiltonian (θS_ϕ) at x- and y-axes for $S = 1$ [36]. $c_{n\theta} = \cos(n\theta)$ and $s_{n\theta} = \sin(n\theta)$.

Angular momentum operator	ϕ	Evolution under the r. f. pulse Hamiltonian
S_x	x	S_x
S_y	x	$S_y c_\theta + S_z s_\theta$
S_z	x	$S_z c_\theta - S_y s_\theta$
$[S_x,S_y]_+$	x	$[S_x,S_y]_+ c_\theta + [S_x,S_z]_+ s_\theta$
$[S_x,S_z]_+$	x	$[S_x,S_z]_+ c_\theta - [S_x,S_z]_+ s_\theta$
$[S_y,S_z]_+$	x	$[S_y,S_z]_+ c_{2\theta} - (S_y^2 - S_z^2) s_{2\theta}$
S_x^2	x	S_x^2
S_y^2	x	$\frac{1}{2}S_y^2(c_{2\theta}+1) - \frac{1}{2}S_z^2(c_{2\theta}-1) + \frac{1}{2}[S_y,S_z]_+ s_{2\theta}$
S_z^2	x	$\frac{1}{2}S_z^2(c_{2\theta}+1) - \frac{1}{2}S_y^2(c_{2\theta}-1) - \frac{1}{2}[S_y,S_z]_+ s_{2\theta}$
S_x	y	$S_x c_\theta - S_z s_\theta$
S_y	y	S_y
S_z	y	$S_z c_\theta + S_x s_\theta$
$[S_x,S_y]_+$	y	$[S_x,S_y]_+ c_\theta + [S_y,S_z]_+ s_\theta$
$[S_x,S_z]_+$	y	$[S_x,S_z]_+ c_{2\theta} + (S_x^2 - S_z^2) s_{2\theta}$
$[S_y,S_z]_+$	y	$[S_y,S_z]_+ c_\theta + [S_x,S_y]_+ s_\theta$
S_x^2	y	$\frac{S_x^2}{2}(c_{2\theta}+1) - \frac{S_z^2}{2}(c_{2\theta}-1) - \frac{1}{2}[S_x,S_z]_+ s_{2\theta}$
S_y^2	y	S_y^2
S_z^2	y	$\frac{S_z^2}{2}(c_{2\theta}+1) - \frac{S_x^2}{2}(c_{2\theta}-1) + \frac{1}{2}[S_x,S_z]_+ s_{2\theta}$

Table 3. Evolutions of nine angular momentum operators under the chemical shift Hamiltonian ($\Omega_S S_z$) for $S = 1$ [36]. $c_{nS} = \cos(n\Omega_S t)$ and $s_{nS} = \sin(n\Omega_S t)$.

Angular momentum operator	Evolution under the chemical shift Hamiltonian
S_x	$S_x c_S + S_y s_S$
S_y	$S_y c_S - S_x s_S$
S_z	S_z
$[S_x,S_y]_+$	$[S_x,S_y]_+ c_{2S} + (S_y^2 - S_x^2) s_{2S}$
$[S_x,S_z]_+$	$[S_x,S_z]_+ c_S + [S_y,S_z]_+ s_S$
$[S_y,S_z]_+$	$[S_y,S_z]_+ c_S - [S_x,S_z]_+ s_S$
S_x^2	$\frac{1}{2}S_x^2(c_{2S}+1) - \frac{1}{2}S_y^2(c_{2S}-1) + \frac{1}{2}[S_x,S_y]_+ s_{2S}$
S_y^2	$\frac{1}{2}S_y^2(c_{2S}+1) - \frac{1}{2}S_x^2(c_{2S}-1) - \frac{1}{2}[S_x,S_y]_+ s_{2S}$
S_z^2	S_z^2

Table 4. Evolutions of 32 product operators under the spin-spin coupling Hamiltonian ($2\pi J I_z S_z$) of the IS ($I = 1/2$, $S = 1$) spin system [36]. $c_{nJ} = \cos(n\pi J t)$ and $s_{nJ} = \sin(n\pi J t)$.

Product operator	Evolution under the spin-spin coupling Hamiltonian
I_x	$I_y S_z s_{2J} + I_x(1 + S_z^2(c_{2J} - 1))$
I_y	$-I_x S_z s_{2J} + I_y(1 + S_z^2(c_{2J} - 1))$
S_x	$S_x c_J + 2I_z S_y s_J$
S_y	$S_y c_J - 2I_z S_x S_J$
$I_x S_z$	$I_x S_z c_{2J} + I_y S_z^2 s_{2J}$
$I_y S_z$	$I_y S_z c_{2J} - I_x S_z^2 s_{2J}$
$I_z S_x$	$I_z S_x c_J + \frac{1}{2} S_y s_J$
$I_z S_y$	$I_z S_y c_J - \frac{1}{2} S_x s_J$
$I_x S_x$	$I_x S_x c_J + I_y [S_x,S_z]_+ s_J$
$I_x S_y$	$I_x S_y c_J + I_y [S_y,S_z]_+ s_J$
$I_y S_x$	$I_y S_x c_J - I_x [S_x,S_z]_+ s_J$
$I_y S_y$	$I_y S_y c_J - I_x [S_y,S_z]_+ s_J$
$I_x S_z^2$	$I_x S_z^2 c_{2J} + I_y S_z s_{2J}$
$I_y S_z^2$	$I_y S_z^2 c_{2J} - I_x S_z s_{2J}$
$I_x S_y^2$	$I_x S_y^2 + \frac{1}{2} I_x S_z^2 (c_{2J} - 1) + \frac{1}{2} I_y S_z s_{2J}$
$I_y S_y^2$	$I_y S_y^2 + \frac{1}{2} I_y S_z^2 (c_{2J} - 1) + \frac{1}{2} I_x S_z s_{2J}$
S_x^2	$\frac{1}{2} S_x^2 (c_{2J} + 1) - \frac{1}{2} S_y^2 (c_{2J} - 1) + I_z [S_y,S_x]_+ s_{2J}$
S_y^2	$\frac{1}{2} S_y^2 (c_{2J} + 1) - \frac{1}{2} S_x^2 (c_{2J} - 1) - I_z [S_y,S_x]_+ s_{2J}$
$I_z S_x^2$	$\frac{1}{2} I_z S_x^2 (c_{2J} + 1) - \frac{1}{2} I_z S_y^2 (c_{2J} - 1) + \frac{1}{4} [S_y,S_x]_+ s_{2J}$
$I_z S_y^2$	$\frac{1}{2} I_z S_y^2 (c_{2J} + 1) - \frac{1}{2} I_z S_x^2 (c_{2J} - 1) - \frac{1}{4} [S_y,S_x]_+ s_{2J}$
$I_x [S_x,S_z]_+$	$I_x [S_x,S_z]_+ c_J + I_y S_x s_J$
$I_x [S_y,S_z]_+$	$I_x [S_y,S_z]_+ c_J + I_y S_y s_J$
$I_y [S_x,S_z]_+$	$I_y [S_x,S_z]_+ c_J - I_x S_x s_J$
$I_y [S_y,S_z]_+$	$I_y [S_y,S_z]_+ c_J - I_x S_y s_J$
$[S_x,S_z]_+$	$[S_x,S_z]_+ c_J + 2I_z [S_y,S_z]_+ s_J$
$[S_y,S_z]_+$	$[S_y,S_z]_+ c_J + 2I_z [S_x,S_z]_+ s_J$
$[S_x,S_y]_+$	$[S_x,S_y]_+ c_{2J} + 2I_z (S_y^2 - S_x^2) s_{2J}$
$I_z [S_x,S_z]_+$	$I_z [S_x,S_z]_+ c_J + \frac{1}{2} \lfloor S_y,S_z \rfloor_+ s_J$
$I_z [S_y,S_z]_+$	$I_z [S_y,S_z]_+ c_J + \frac{1}{2} [S_x,S_z]_+ s_J$
$I_z [S_x,S_y]_+$	$I_z [S_x,S_y]_+ c_{2J} + \frac{1}{2} (S_y^2 - S_x^2) s_{2J}$
$I_x S_x^2$	$I_x S_x^2 + \frac{1}{2} I_x S_z^2 (c_{2J} - 1) + \frac{1}{2} I_y S_z s_{2J}$
$I_y S_x^2$	$I_y S_x^2 + \frac{1}{2} I_y S_z^2 (c_{2J} - 1) - \frac{1}{2} I_x S_z s_{2J}$

illustrated in Fig. 1, is used [3], where the density matrix operator at each stage of the experiment is labelled with numbers. ^{13}C is treated as spins I and I', and ^{2}H(D) as spins S and S' in Figure 1. In the pulse sequence, the optimum value of Δ is $1/(2J_{IS})$, Δ' is a short compensation delay, t_1 is the incremented evolution delay during homonuclear spin-spin coupling, which takes place between S and S' spins and t_2 is the acquisition time for S and S' spins along y-axes [3]. Starting from the density matrix operator at thermal equilibrium, one should apply the required Hamiltonians during the pulse sequence and obtain the density matrix operator at the end of the experiment. For this experiment, r. f. pulse, chemical shift and spin-spin coupling Hamiltonians are applied. For $I = I' = \frac{1}{2}$ spins, evolutions of angular momentum operators under the r. f. pulse Hamiltonian are known [12, 22]. In the case of $S = S' = 1$ spins, evolutions of 9 angular momentum operators under the r. f. pulse Hamiltonian were obtained in our previous study [36]. They are presented in Table 2. During t_2, the chemical shift Hamiltonian for angular momentum operators of $S = S' = 1$ spins is applied. Their evolutions are presented in Table 3 [36]. During Δ and Δ', the spin-spin coupling Hamiltonians $\mathcal{H}_J(I-S) = 2\pi J_{IS} I_z S_z$ and $\mathcal{H}'_J(I'-S') = 2\pi J_{I'S'} I'_z S'_z$ are applied to the IS ($I = \frac{1}{2}$, $S = 1$) and

$I'S'$ ($I' = \frac{1}{2}$, $S' = 1$) spin systems, respectively. For these spin systems, evolutions of 36 (or 40 in separated form) product operators under the spin-spin coupling Hamiltonian are known and given in Table 4 [36]. During t_1, the homonuclear spin-spin coupling Hamiltonian $\mathcal{H}_J(S-S') = 2\pi J_{SS'}S_zS'_z$ is applied to the SS' ($S = 1$, $S' = 1$) spin system. Required evolutions are obtained in Section 3. For multi-spin systems, to follow these processes (applications of required Hamiltonians during the pulse sequence) by hand becomes too difficult. In order to overcome this problem a computer program is written in Mathematica for the present study. This program is used to obtain the density matrix operator at the end of the experiment for different spin systems.

For the $ISI'S'$ multi-spin system, the density matrix at thermal equilibrium is $\sigma_0 = S_z + S'_z$. By using the computer program the following density matrices for each labelled point are obtained:

$$\sigma_0 \xrightarrow{90^\circ_x(S,S')} -S_y - S'_y \equiv \sigma_1, \tag{14}$$

$$\sigma_1 \xrightarrow{2\pi J_{IS}I_zS_z\Delta(\Delta=1/(2J_{IS}))+2\pi J_{I'S'}I'_zS'_z\Delta(\Delta=1/(2J_{I'S'}))} 2I_zS_x + 2I'_zS'_x, \tag{15}$$

$$\sigma_2 \xrightarrow{180^\circ_x(S,S')+90^\circ_x(I,I')} -2I_yS_x - 2I'_yS'_x, \tag{16}$$

$$\sigma_3 \xrightarrow{2\pi J_{IS}I_zS_z\Delta(\Delta=1/(2J_{IS}))+2\pi J_{I'S'}I'_zS'_z\Delta(\Delta=1/(2J_{I'S'}))} 2I_xS_{xz} + 2I'_xS'_{xz}, \tag{17}$$

$$\sigma_4 \xrightarrow{90^\circ_x(S,S')} -2I_xS_{xy} - 2I'_xS'_{xy} \equiv \sigma_5, \tag{18}$$

$$\begin{aligned}\sigma_{16} = {} & -Syc_Ss_\theta - S'_yc'_Ss_\theta + S_yS'^2_zs_\theta + S^2_zS'_yc'_Ss_\theta \\ & - S_yS'^2_zc_{2J}c_Ss_\theta - S^2_zS'_yc'_{2J}c'_Ss_\theta + 2I_xS_{xy}c_\theta \\ & + 2I'_xS'_{xy}c_\theta + 2I_xS_{xy}S'^2_zc_\theta + 2I'_xS'_{xy}S^2_zc_\theta \\ & + 2I_xS_{xy}S'^2_zc_{4J}c_\theta + 2I'_xS'_{xy}S^2_zc'_{4J}c_\theta \\ & - 2I_xS^2_xS'_zs_{4J}c_{2S}c_\theta - 2I_xS'^2_xS_zs'_{4J}c_{2S}c_\theta \\ & + 2I_xS^2_yS'_zs_{4J}c_{2S}c_\theta + 2I_xS'^2_yS_zs'_{4j}c_{2S}c_\theta \\ & + S_xS'_zs_{2J}c_Ss_\theta + S_zS'_xs'_{2J}c_Ss_\theta + S_xs_Ss_\theta \\ & + S'_xs_Ss_\theta - S_xS'^2_zs_Ss_\theta - S^2_zS'_xs_Ss_\theta \\ & + S_xS'^2_zc_{2J}s_Ss_\theta + S^2_zS'_xc'_{2J}s_Ss_\theta \\ & + S_zS'_ys_{2J}s_Ss_\theta + S_yS'_zs'_{2j}s_Ss_\theta \\ & - 2I_xS_{xy}S'_zs_{4J}s_{2S}c_\theta - 2I'_xS'_{xy}S_zs'_{4j}s_{2S}c_\theta,\end{aligned} \tag{19}$$

where $c_{nJ} = \cos(n\pi J_{SS'}t_1)$, $c'_{nJ} = \cos(n\pi J'_{S'S}t_1)$, $s_{nJ} = \sin(n\pi J_{SS'}t_1)$, $s'_{nJ} = \sin(n\pi J'_{S'S}t_1)$, $c_{nS} = \cos(n\Omega_St_2)$, $c'_{nS} = \cos(n\Omega'_St_2)$, $s_{nS} = \sin(n\Omega_St_2)$, $s'_{nS} = \sin(n\Omega'_St_2)$, $S_{xz} = [S_x,S_z]_+$, $S_{yz} = [S_y,S_z]_+$, $S_{xy} = [S_x,S_y]_+$, $S'_{xz} = [S'_x,S'_z]_+$, $S'_{yz} = [S'_y,S'_z]_+$ and $S'_{xy} = [S'_x,S'_y]_+$. In the density matrix operator, only the terms with observable product operators are kept as they are the only ones that contribute to the signal on *y*-axis detection. Then the magnetization along the *y*-axis is proportional to $\langle S_y\rangle + \langle S'_y\rangle$ and

$$M_y(t_1t_2) \propto \langle S_y\rangle + \langle S'_y\rangle = \mathrm{Tr}[S_y\sigma_{16}] + \mathrm{Tr}[S'_y\sigma_{16}]. \tag{20}$$

Now it is necessary to obtain the $\mathrm{Tr}[S_yO]$ and $\mathrm{Tr}[S'_yO']$ values of observable product operators indicated by O and O'. These trace values are calculated by a computer program in Mathematica and the results for several multi-spin systems are given in Tables 5 and 6. For example, trace of the S_y product operator is calculated as

$$\begin{aligned}\mathrm{Tr}[S_{iy}O] &= \mathrm{Tr}[S_yS_y] \\ &= \mathrm{Tr}[(E_1\otimes S_y\otimes E'_1\otimes E'_S)\cdot(E_1\otimes S_y\otimes E'_1\otimes E'_S)] \\ &= 24.\end{aligned} \tag{21}$$

By using Tables 5 and 6,

$$\langle S_y\rangle + \langle S'_y\rangle = -8(1+2c_{2J})c_Ss_\theta - 8(1+2c'_{2J})c'_Ss_\theta \tag{22}$$

is obtained for the $ISI'S'$ multi-spin system. This equation represents the FID signals of the 2D MAXY-*J*RES NMR experiment for the $ISI'S'$ multi-spin system. There exist triplet signals with the same intensity distribution of $1:1:1$ for both S and S' spins at the coordinates $(2J,\Omega_S):(\Omega_S):(-2J,\Omega_S)$ and $(2J',\Omega'_S):(\Omega'_S):(-2J',\Omega'_S)$, respectively. Another example can be the $IS_2I'S'$ multi-spin system. As one can guess, product operator calculations for this spin system will be more complicated than those of the $ISI'S'$ multi-spin system. The product operator description of this spin system is provided in Appendix B.

For the $ISI'S'$, $IS_2I'S'$, $IS_3I'S'$, $IS_2I'S'_2$ and $IS_3I'S'_2$ multi-spin systems, the trace values of the density matrix operators and their signal coordinates with the intensity distributions are given in Tables 7 and 8 for S and S' spins, respectively.

$\sum_{i=1}^{n}\mathrm{Tr}[S_{iy}\sigma_{16}] + \sum_{j=1}^{m}\mathrm{Tr}[S'_{jy}\sigma_{16}]$ values obtained for the $ISI'S'$, $IS_2I'S'$, $IS_3I'S'$, $IS_2I'S'_2$ and $IS_3I'S'_2$ multi-spin systems represent the FID signals of the 2D MAXY-*J*RES NMR experiment of CDCD, $\mathrm{CD_2CD}$, $\mathrm{CD_3CD}$, $\mathrm{CD_2CD_2}$ and $\mathrm{CD_3CD_2}$ groups,

Table 5. Results of the $\sum_{i=1}^{n}\mathrm{Tr}[S_{iy}O]$ calculations for observable product operators of $IS_nI'S'_m$ multi-spin systems ($k=x,y,z$; $l=x,y,z$; $o=x,y,z$; $p=x,y,z$).

Spin system	Product operators (O)	$\sum_{i=1}^{n}\mathrm{Tr}[S_{iy}O]$
$ISI'S'$	S_y	24
	$S_yS'^2_k$	16
$IS_2I'S'$	$S_{1y}+S_{2y}$	144
	$S_{1y}(S^2_{2k}+S'^2_k)+S_{2y}(S^2_{1k}+S'^2_k)$	192
	$S_{1y}S^2_{2k}S'^2_I+S^2_{1k}S_{2y}S'^2_I$	64
$IS_3I'S'$	$S_{1y}+S_{2y}+S_{3y}$	648
	$S_{1y}(S^2_{2k}+S^2_{3k}+S'^2_k)+S_{2y}(S^2_{1k}+S^2_{3k}+S'^2_k)+S_{3y}(S^2_{1k}+S^2_{2k}+S'^2_k)$	1296
	$S_{1y}(S^2_{2k}S^2_{3I}+S^2_{2k}S'^2_I+S^2_{3k}S'^2_I)+S_{2y}(S^2_{1k}S^2_{3I}+S^2_{1k}S'^2_I+S^2_{3k}S'^2_I)+S_{3y}(S^2_{1k}S^2_{2I}+S^2_{1k}S'^2_I+S^2_{2k}S'^2_I)$	864
	$S_{1y}S^2_{2k}S^2_{3l}S'^2_o+S^2_{1k}S_{2y}S^2_{3l}S'^2_o+S^2_{1k}S^2_{2l}S_{3y}S'^2_o$	192
$IS_2I'S'_2$	$S_{1y}+S_{2y}$	432
	$S_{1y}(S^2_{2k}+S'^2_{1k}+S'^2_{2k})+S_{2y}(S^2_{1k}+S'^2_{1k}+S'^2_{2k})$	864
	$S_{1y}(S^2_{2k}S'^2_{1l}+S^2_{2k}S'^2_{2l}+S'^2_{1k}S'^2_{2l})+S_{2y}(S^2_{1k}S'^2_{1l}+S^2_{1k}S'^2_{2l}+S'^2_{1k}S'^2_{2l})$	576
	$S_{1y}S^2_{2k}S'^2_{1l}S'^2_{2o}+S^2_{1k}S_{2y}S'^2_{1l}S'^2_{2o}$	128
$IS_3I'S'_2$	$S_{1y}+S_{2y}+S_{3y}$	1944
	$S_{1y}(S^2_{2k}+S^2_{3k}+S'^2_{1k}+S'^2_{2k})+S_{2y}(S^2_{1k}+S^2_{3k}+S'^2_{1k}+S'^2_{2k})+S_{3y}(S^2_{1k}+S^2_{2k}+S'^2_{1k}+S'^2_{2k})$	5184
	$S_{1y}(S^2_{2k}S^2_{3l}+S^2_{2k}S'^2_{1l}+S^2_{2k}S'^2_{2l}+S^2_{3k}S'^2_{1l}+S^2_{3k}S'^2_{2l}+S'^2_{1k}S'^2_{2l})+S_{2y}(S^2_{1k}S^2_{3l}+S^2_{1k}S'^2_{1l}+S^2_{1k}S'^2_{2l}+S^2_{3k}S'^2_{1l}+S^2_{3k}S'^2_{2l}+$ $S'^2_{1k}S'^2_{2l})+S_{3y}(S^2_{1k}S^2_{2l}+S^2_{1k}S'^2_{1l}+S^2_{1k}S'^2_{2l}+S^2_{2k}S'^2_{1l}+S^2_{2k}S'^2_{2l}+S'^2_{1k}S'^2_{2l})$	5184
	$S_{1y}(S^2_{2k}S^2_{3l}S'^2_{1o}+S^2_{2k}S^2_{3l}S'^2_{2o}+S^2_{2k}S'^2_{1l}S'^2_{2o}+S^2_{3k}S'^2_{1l}S'^2_{2o})+S_{2y}(S^2_{1k}S^2_{3l}S'^2_{1o}+S^2_{1k}S^2_{3l}S'^2_{2o}+S^2_{1k}S'^2_{1l}S'^2_{2o}+S^2_{3k}S'^2_{1l}S'^2_{2o})+$ $S_{3y}(S^2_{1k}S^2_{2l}S'^2_{1o}+S^2_{1k}S^2_{2l}S'^2_{2o}+S^2_{1k}S'^2_{1l}S'^2_{2o}+S^2_{2k}S'^2_{1l}S'^2_{2o})$	2304
	$S_{1y}S^2_{2k}S^2_{3l}S'^2_{1o}S'^2_{2p}+S^2_{1k}S_{2y}S^2_{3l}S'^2_{1o}S'^2_{2p}+S^2_{1k}S^2_{2l}S_{3y}S'^2_{1o}S'^2_{2p}$	384

Table 6. Results of the $\sum_{j=1}^{m}\mathrm{Tr}[S'_{jy}O']$ calculations for observable product operators of $IS_nI'S'_m$ multi-spin systems ($k=x,y,z$; $l=x,y,z$; $o=x,y,z$; $p=x,y,z$).

Spin system	Product operators (O)	$\sum_{j=1}^{n}\mathrm{Tr}[S'_{jy}O']$
$ISI'S'$	S'_y	24
	$S^2_kS'_y$	16
$IS_2I'S'$	S'_y	72
	$(S^2_{1k}+S^2_{2k})S'_y$	96
	$S^2_{1k}S^2_{2l}S'_y$	32
$IS_3I'S'$	S'_y	216
	$(S^2_{1k}+S^2_{2k}+S^2_{3k})S'_y$	432
	$(S^2_{1k}S^2_{2l}+S^2_{1k}S^2_{3l}+S^2_{2k}S^2_{3l})S'_y$	288
	$S^2_{1k}S^2_{2l}S^2_{3o}S'_y$	64
$IS_2I'S'_2$	$S'_{1y}+S'_{2y}$	432
	$(S^2_{1k}+S^2_{2k}+S'^2_{2k})S'_{1y}+(S^2_{1k}+S^2_{2k}+S'^2_{1k})S'_{2y}$	864
	$(S^2_{1k}S^2_{2l}+S^2_{1k}S'^2_{2l}+S^2_{2k}S'^2_{2l})S'_{1y}+(S^2_{1k}S^2_{2l}+S^2_{1k}S'^2_{1l}+S^2_{2k}S'^2_{1l})S'_{2y}$	576
	$S^2_{1k}S^2_{2l}S'_{1y}S'^2_{2o}+S^2_{1k}S^2_{2l}S'^2_{1o}S'_{2y}$	128
$IS_3I'S'_2$	$S'_{1y}+S'_{2y}$	1296
	$(S^2_{1k}+S^2_{2k}+S^2_{3k}+S'^2_{2k})S'_{1y}+(S^2_{1k}+S^2_{2k}+S^2_{3k}+S'^2_{1k})S'_{2y}$	3456
	$(S^2_{1k}S^2_{2l}+S^2_{1k}S^2_{3l}+S^2_{2k}S^2_{3l}+S^2_{1k}S'^2_{2l}+S^2_{2k}S'^2_{2l}+S^2_{3k}S'^2_{2l})S'_{1y}+(S^2_{1k}S^2_{2l}+S^2_{1k}S^2_{3l}+S^2_{2k}S^2_{3l}+S^2_{1k}S'^2_{1l}+S^2_{2k}S'^2_{1l}+$ $S^2_{3k}S'^2_{1l})S'_{2y}$	3456
	$(S^2_{1k}S^2_{2l}S^2_{3o}+S^2_{1k}S^2_{2l}S'^2_{2o}+S^2_{1k}S^2_{3l}S'^2_{2o}+S^2_{2k}S^2_{3l}S'^2_{2o})S'_{1y}+(S^2_{1k}S^2_{2l}S^2_{3o}+S^2_{1k}S^2_{2l}S'^2_{1o}+S^2_{1k}S^2_{3l}S'^2_{1o}+S^2_{2k}S^2_{3l}S'^2_{1o})S'_{2y}$	1536
	$S^2_{1k}S^2_{2l}S^2_{3o}S'_{1y}S'^2_{2p}+S^2_{1k}S^2_{2l}S^2_{3o}S'^2_{1p}S'_{2y}$	256

respectively. The $\sum_{i=1}^{n}\mathrm{Tr}[S_{iy}\sigma_{16}]+\sum_{j=1}^{m}\mathrm{Tr}[S'_{jy}\sigma_{16}]$ values for $IS_nI'S'_m$ ($I=I'=\frac{1}{2}$; $S=S'=1$; $n=1,2,3$; $m=1,2$) multi-spin systems can be generalized as follows:

$$\sum_{i=1}^{n}\mathrm{Tr}[S_{iy}\sigma_{16}]+\sum_{j=1}^{m}\mathrm{Tr}[S'_{jy}\sigma_{16}](IS_nI'S'_m)=$$

Table 7. $\sum_{i=1}^{n} \mathrm{Tr}[S_{iy}\sigma_{16}]$ values, signal coordinates and intensity distribution for S spins of various multi-spin systems.

Spin system	$\sum_{i=1}^{n} \mathrm{Tr}[S_{iy}\sigma_{16}]$	Signal coordinate	Intensity distribution
$ISI'S'$	$-8(1+3c_{2J})c_S s_\theta$	$(2J,\Omega_S):(\Omega_S):(-2J,\Omega_S)$	1 : 1 : 1
$IS_2I'S'$	$-16(1+2c_{2J})c_S(1-2c_\theta)s_\theta$	$(2J,\Omega_S):(\Omega_S):(-2J,\Omega_S)$	1 : 1 : 1
$IS_3I'S'$	$-24(1+2c_{2J})c_S(1-2c_\theta)^2 s_\theta$	$(2J,\Omega_S):(\Omega_S):(-2J,\Omega_S)$	1 : 1 : 1
$IS_2I'S'_2$	$-16(1+2c_{2J})^2 c_S(1-2c_\theta)s_\theta$	$(4J,\Omega_S):(2J,\Omega_S):(\Omega_S):(-2J,\Omega_S):(-4J,\Omega_S)$	1 : 2 : 3 : 2 : 1
$IS_2I'S'_2$	$-24(1+2c_{2J})^2 c_S(1-2c_\theta)^2 s_\theta$	$(4J,\Omega_S):(2J,\Omega_S):(\Omega_S):(-2J,\Omega_S):(-4J,\Omega_S)$	1 : 2 : 3 : 2 : 1

Table 8. $\sum_{j=1}^{m} \mathrm{Tr}[S'_{jy}\sigma_{16}]$ values, signal coordinates and intensity distribution for S' spins of various multi-spin systems.

Spin system	$\sum_{j=1}^{m} \mathrm{Tr}[S'_{jy}\sigma_{16}]$	Signal coordinate	Intensity distribution
$ISI'S'$	$-8(1+2c'_{2J})c'_S s_\theta$	$(2J,\Omega'_S):(\Omega'_S):(-2J,\Omega'_S)$	1 : 1 : 1
$IS_2I'S'$	$-8(1+2c'_{2J})^2 c'_S s_\theta$	$(4J,\Omega'_S):(2J,\Omega'_S):(\Omega'_S):(-2J,\Omega'_S):(-4J,\Omega'_S)$	1 : 2 : 3 : 2 : 1
$IS_3I'S'$	$-8(1+2c'_{2J})^3 c'_S s_\theta$	$(6J,\Omega'_S):(4J,\Omega'_S):(2J,\Omega'_S):(\Omega'_S):(-2J,\Omega'_S):(-4J,\Omega'_S):(-6J,\Omega'_S)$	1 : 3 : 6 : 7 : 6 : 3 : 1
$IS_2I'S'_2$	$-16(1+2c'_{2J})^2 c'_S(1-2c_{2\theta})s_\theta$	$(4J,\Omega'_S):(2J,\Omega'_S):(\Omega'_S):(-2J,\Omega'_S):(-4J,\Omega'_S)$	1 : 2 : 3 : 2 : 1
$IS_3I'S'_2$	$-16(1+2c'_{2J})^3 c'_S(1-2c_{2\theta})s_\theta$	$(6J,\Omega'_S):(4J,\Omega'_S):(2J,\Omega'_S):(\Omega'_S):(-2J,\Omega'_S):(-4J,\Omega'_S):(-6J,\Omega'_S)$	1 : 3 : 6 : 7 : 6 : 3 : 1

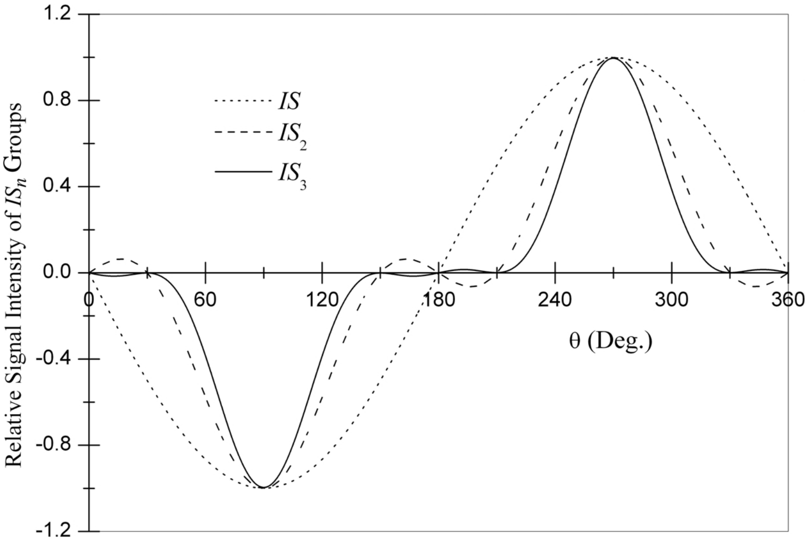

Fig. 2. Plots of relative signal intensity of 2D ^{2}H MAXY-*J*RES NMR spectroscopy of IS_n groups as functions of the selective pulse angle θ.

$$-8n(1+2c_{2J})^m c_S(1-2c_{2\theta})^{n-1}s_\theta - 8m(1+2c_{2J})^n c'_S(1-2c_{2\theta})^{m-1}s_\theta. \quad (23)$$

The $\sum_{i=1}^{n} \mathrm{Tr}[S_{iy}\sigma_{16}] + \sum_{j=1}^{m} \mathrm{Tr}[S'_{jy}\sigma_{16}]$ values can be normalized by multiplication of the first term with $36/(8nm\mathrm{Tr}(E))$ and the second term with $36/(8mn\mathrm{Tr}(E'))$. Here E and E' is the unity product operator of the corresponding spin system. So, normalized FID values can be also generalized as follows:

$$\sum_{i=1}^{n} \mathrm{Tr}[S_{iy}\sigma_{16}] + \sum_{j=1}^{m} \mathrm{Tr}[S'_{jy}\sigma_{16}] = -\frac{1}{m}\frac{1}{3^{n+m-2}}(1+2c_{2J})^m c_S(1-2c_{2\theta})^{n-1}s_\theta - \frac{1}{n}\frac{1}{3^{n+m-2}}(1+2c_{2J})^n c'_S(1-2c_{2\theta})^{m-1}s_\theta. \quad (24)$$

The plots of these normalized and generalized functions of 2D ^{2}H MAXY-*J*RES NMR spectroscopy are presented in Figure 2. As can be seen in this figure, the relative signal intensities of the IS, IS_2 and IS_3 groups vary as functions of the selective pulse angle θ.

4.2. Experimental Suggestions and Simulated Spectra

The real relative signal intensities of the 2D MAXY-*J*RES NMR experiment for CD_n groups are given in Table 9. As can be seen in Table 9 and in Fig. 2, for θ = 195° or 345°, while CD and CD_3 groups are giving positive signals CD_2 groups give negative signals. When the experiment is performed for angles of 210° or 330°, positive signals are only observed for

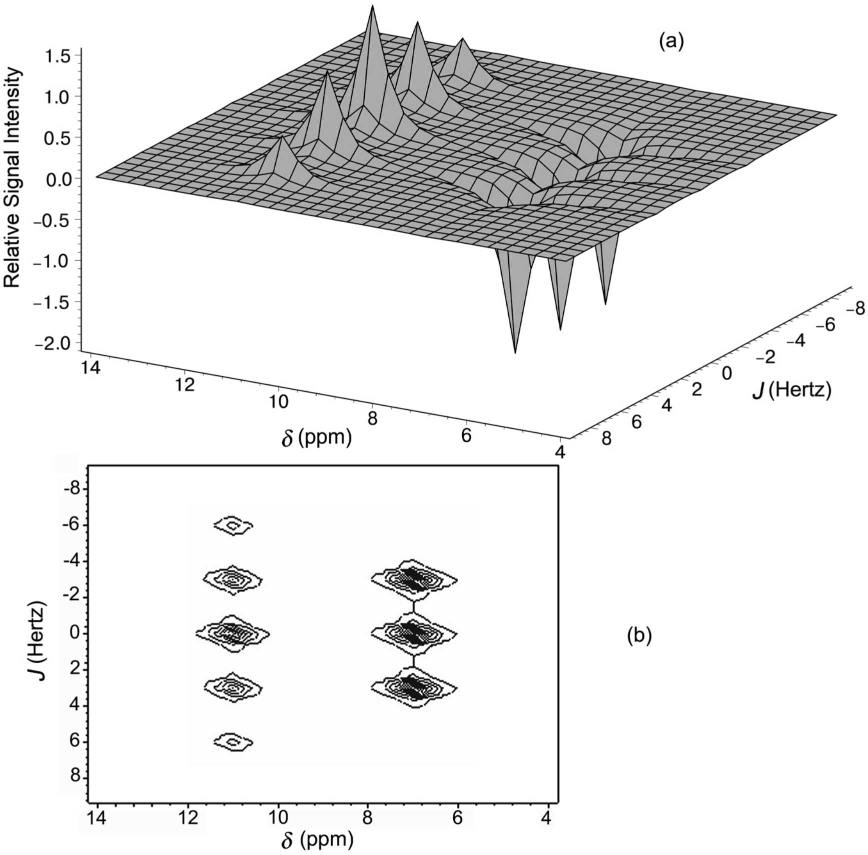

Fig. 3. Simulated 2D ^{2}H MAXY-*J*RES NMR spectrum of the CD_2CD group for $\theta = 195°$.

Table 9. Real relative signal intensities of the 2D MAXY-*J*RES NMR experiment of CD_n groups for several pulse angles θ.

Spin system	$\theta = 195°$ or 345°	$\theta = 210°$ or 330°	$\theta = 225°$ or 315°	$\theta = 270°$
IS(CD)	0.259	0.5	0.707	1
$IS_2(CD_2)$	−0.379	0	1.414	6
$IS_3(CD_3)$	0.416	0	2.121	27

CD groups. For the angle of 270°, all groups, CD, CD_2 and CD_3, give positive signals with the real relative signal intensities of 1, 6 and 27, respectively. When the pulse angle is 225° or 315°, real relative signal intensities of the CD, CD_2 and CD_3 groups are 0.707, 1.414 and 2.121, respectively. By comparing their real relative signal intensities obtained for the angles of 195°, 210° and 270°, one can easily distinguish CD, CD_2 and CD_3 groups from each other. After these identifications, the splitting of signals in the spectra of the 2D MAXY-*J*RES NMR experiment can be used for the identification of neighbour ^{2}H nuclei. The explanation for this is given as follows.

For product operator description and spectrum simulation of multiple-pulse NMR experiments, a computer program was written by Kanters et al. [37, 38]. This is called Product Operator Formalism using Maple (POF.M). In order to obtain the simulated spectra, POF.M is implemented for Fourier transformation of our obtained theoretical results. In simulated spectra of CD_nCD_m groups, chemical shifts of ^{2}H nuclei are set to be 11, 7 and 3 ppm for CD, CD_2 and CD_3 groups, respectively. Spin-spin coupling constants between two ^{2}H nuclei are assumed to be 3, 4 and 5 Hz in CD_2CD, CD_3CD and CD_3CD_2 groups, respectively. For the angle $\theta = 195°$, the simulated spectrum of the CD_2CD group is presented in Fig. 3; three negative signals $(-1:-1:-1)$ and five positive signals $(1:2:3:2:1)$ for CD_2 and CD groups, respectively, can be observed. In Fig. 4, the simulated spectrum of the CD_3CD group is given for $\theta = 210°$. For this angle, as expected, only the CD group gives seven positive signals with an intensity distribution of $1:3:6:7:6:3:1$. For the

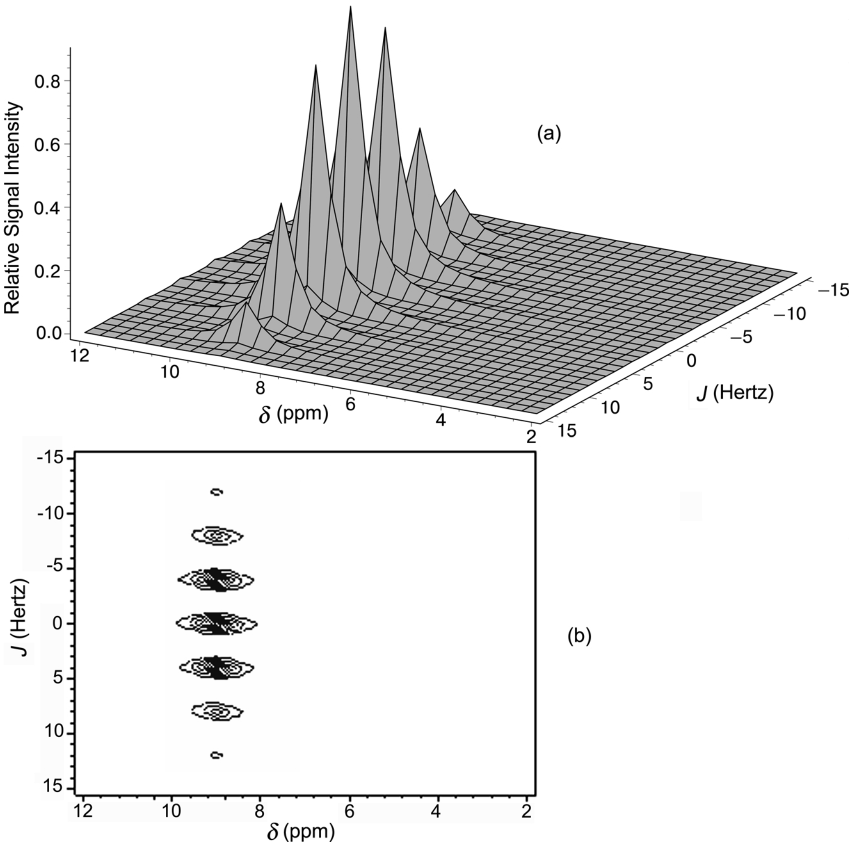

Fig. 4. Simulated 2D ^{2}H MAXY-*J*RES NMR spectrum of the CD_3CD group for $\theta = 210^\circ$.

CD_3CD_2 group, the simulated spectrum for $\theta = 270^\circ$ is presented in Figure 5. For this angle, both CD_3 (five signals with an intensity distribution of $1:2:3:2:1$) and CD_2 (seven signals with intensities of $1:3:6:7:6:3:1$) groups give maximum positive signals.

5. Conclusion

The 2D MAXY-*J*RES NMR experiment is a combination of MAXY and homonuclear *J*-resolved NMR spectroscopy. This technique is used for the identification of CH_nCH_m groups in complex samples. In this study, first, evolutions of some product operators under the homonuclear scalar spin-spin coupling Hamiltonian for an SS' ($S = 1, S' = 1$) spin system are obtained. Then, by using the product operator theory, analytical descriptions of the 2D MAXY-*J*RES experiment for $IS_nI'S'_m$ ($I = I' = \frac{1}{2}$; $S = S' = 1$; $n = 1,2,3$; $m = 1,2$) multi-spin systems are presented. The obtained results for each CD_nCD_m group represent the FID signals of this experiment. By using these results experimental suggestions are made and simulated spectra are obtained for various CD_nCD_m groups. As a result, it is shown that the 2D MAXY-*J*RES NMR experiment can be used to distinguish CD, CD_2 and CD_3 groups from each other in CD_nCD_m systems.

Appendix A: Complete Product Operator Theory for the *IS* ($I = 1/2, S = 1$) Spin System

The complete product operator for the *IS* ($I = 1/2$, $S = 1$) spin system is presented in our previous study [36]. For this spin system, evolutions of nine angular momentum operators of spin $S = 1$ under r. f. pulse and chemical shift Hamiltonians were obtained, and they are given in Tables 2 and 3, respectively. For the *IS* ($I = 1/2$, $S = 1$) spin system evolutions of 32 product operators under the spin-spin coupling Hamiltonian are given in Table 4. The rest 8 product operators of E, I_z, I_zS_z, S_z, S_z^2, $I_zS_z^2$, $I_x[S_x,S_y]_+$ and $I_y[S_x,S_y]_+$ do not change under the spin-spin coupling Hamiltonian.

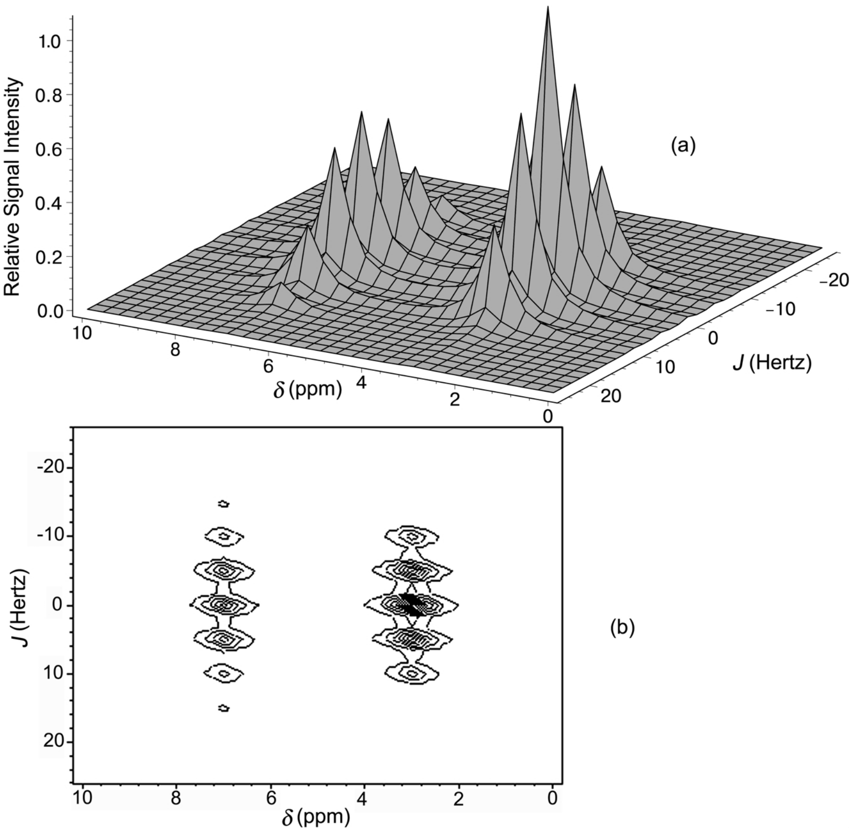

Fig. 5. Simulated 2D ^{2}H MAXY-*J*RES NMR spectrum of the CD_3CD_2 group for $\theta = 270°$.

Appendix B: Product Operator Description of the 2D MAXY-*J*RES NMR Experiment for the $IS_2I'S'$ Multi-Spin System

For the $IS_2I'S'$ multi-spin system, the density matrix at thermal equilibrium is $\sigma_0 = S_{1z} + S_{2z} + S'_z$. By using the computer program the following density matrices for each labelled point are obtained:

$$\sigma_0 \xrightarrow{90^\circ_x(S_1,S_2,S')} -S_{1y} - S_{2y} - S'_y \equiv \sigma_1, \tag{B1}$$

$$\sigma_1 \xrightarrow{(\mathcal{H}_{1J}+\mathcal{H}_{2J})\Delta(\Delta=1/(2J_{IS}))+\mathcal{H}'_J\Delta(\Delta=1/(2J_{I'S'}))} 2I_zS_{1x} + 2I_zS_{2x} + 2I'_zS'_x, \tag{B2}$$

$$\sigma_2 \xrightarrow{180^\circ_x(S_1,S_2,S')+90^\circ_x(I,I')} -2I_yS_{1x}-2I_yS_{2x}-2I'_yS'_x, \tag{B3}$$

$$\sigma_3 \xrightarrow{(\mathcal{H}_{1J}+\mathcal{H}_{2J})\Delta(\Delta=1/(2J_{IS}))+\mathcal{H}'_J\Delta(\Delta=1/(2J_{I'S'}))} 2I_xS_{1xz} + 2I_xS_{2xz} + 2I'_xS'_{xz}, \tag{B4}$$

$$\sigma_4 \xrightarrow{90^\circ_x(S_1,S_2,S')} -2I_xS_{1xy} - 2I_xS_{2xy} - 2I'_xS'_{xy} \equiv \sigma_5, \tag{B5}$$

$$\begin{aligned}\sigma_{16} = {} & \frac{1}{2}(-2A+B+2C-D)c_Ss_\theta \\ & + \frac{1}{2}(-2C+D)c_{2J}c_Ss_\theta + \frac{1}{2}(B-D)c_Sc_{2\theta}s_\theta \\ & + \frac{1}{2}Dc_{2J}c_Sc_{2\theta}s_\theta \\ & + \frac{1}{2}D'(c_{2J}c_{4J}c_Sc_{2S}s_\theta + c_{2J}c_{4J}c_Sc_{2S}c_{2\theta}s_\theta) \\ & + \frac{1}{2}(B'-D')(c_Sc_{2S}c_{2\theta}s_\theta + c_{4J}c_Sc_{2S}c_{2\theta}s_\theta \\ & \qquad + c_Sc_{2S}s_\theta + c_{4J}c_Sc_{2S}s_\theta) \\ & - D's_{2J}s_{4J}c_Sc_{2S}c_\theta s_{2\theta} + (-F+G-H)c'_Ss_\theta \\ & - (G+H)c_{2J}c'_ss_\theta - Hc^2_{2J}c'_Ss_\theta,\end{aligned} \tag{B6}$$

where

$$A = S_{1y} + S_{2y}, \tag{B7}$$

$$B = S_{1y}(S^2_{2x} + S^2_{2y}) + (S^2_{1x} + S^2_{1y})S_{2y}, \tag{B8}$$

$$B' = S_{1y}(S^2_{2x} - S^2_{2y}) + (S^2_{1x} - S^2_{1y})S_{2y}, \tag{B9}$$

$$C = S_{1y}S_z'^2 + S_{2y}S_z'^2, \tag{B10}$$

$$D = S_{1y}(S_{2x}^2 S_z'^2 + S_{2y}^2 S_z'^2) + (S_{1x}^2 + S_{1y}^2)S_{2y}S_z'^2, \tag{B11}$$

$$D' = S_{1y}(S_{2x}^2 S_z'^2 - S_{2y}^2 S_z'^2) + (S_{1x}^2 - S_{1y}^2)S_{2y}S_z'^2, \tag{B12}$$

$$F = S_y', \tag{B13}$$

$$G = S_{1z}^2 S_y' + S_{2z}^2 S_y', \tag{B14}$$

$$H = S_{1z}^2 S_{2z}^2 S_y'. \tag{B15}$$

Also in (B1) – (B6), $\mathcal{H}_{1J} = 2\pi J I_z S_{1z}$, $\mathcal{H}_{2J} = 2\pi J I_z S_{2z}$, and $\mathcal{H}_J' = 2\pi J I_z' S_z'$. In the density matrix operator, only the terms with observable product operators are kept, as they are the only ones that contribute to the signal on y-axis detection. Then the magnetization along the y-axis is proportional to $\langle S_{1y} + S_{2y}\rangle + \langle S_y'\rangle$ and

$$M_y(t_1,t_2) \propto \langle S_{1y} + S_{2y}\rangle + \langle S_y'\rangle = \mathrm{Tr}[(S_{1y} + S_{2y})\sigma_{16}] + \mathrm{Tr}[S_y'\sigma_{16}]. \tag{B16}$$

Now it is necessary to obtain the $\mathrm{Tr}[(S_{1y} + S_{2y})O]$ and $\mathrm{Tr}[S_y'O']$ values of the observable product operators indicated by O and O'. These trace values are calculated by a computer program in Mathematica, and the results for several multi-spin systems are given in Tables 5 and 6. For example, the trace value of the $S_{1y} + S_{2y}$ product operator for the $IS_2I'S'$ multi-spin system is calculated as

$$\begin{aligned}\sum_{i=1}^{2} \mathrm{Tr}[S_{iy}O] &= \mathrm{Tr}[S_{1y}S_{1y}] + \mathrm{Tr}[S_{2y}S_{2y}] \\ &= \mathrm{Tr}[(E_I \otimes S_{1y} \otimes E_{2S} \otimes E_I' \otimes E_s') \\ &\quad \cdot (E_I \otimes S_{1y} \otimes E_{2S} \otimes E_I' \otimes E_s')] \\ &\quad + \mathrm{Tr}[(E_I \otimes E_{1S} \otimes S_{2y} \otimes E_I' \otimes E_s') \\ &\quad \cdot (E_I \otimes E_{1S} \otimes S_{2y} \otimes E_I' \otimes E_s') \\ &= 144.\end{aligned} \tag{B17}$$

By using Tables 5 and 6,

$$\begin{aligned}\langle S_{1y} + S_{2y}\rangle + \langle S_y'\rangle = &-16(1 + 2c_{2J})c_S(1 - 2c_{2\theta})s_\theta \\ &- 8(1 + 2c_{2J})^2 c_S' s_\theta\end{aligned} \tag{B18}$$

is obtained for the $IS_2I'S'$ multi-spin system. This equation represents the FID signals of the 2D MAXY-*J*RES NMR experiment for the $IS_2I'S'$ multi-spin system. There exists triplet signals at $(2J,\Omega_S') : (\Omega_S) : (-2J,\Omega_S)$ coordinates with the intensity distribution of 1 : 1 : 1 for the S spin and five signals at $(4J,\Omega_S') : (2J,\Omega_S') : (\Omega_S') : (-2J,\Omega_S') : (-4J,\Omega_S')$ coordinates with the intensity distribution of 1 : 2 : 3 : 2 : 1 for the S' spin.

[1] M. Liu, R. D. Farrant, J. K. Nicholson, and J. C. Lindon, J. Magn. Reson. Series B **106**, 270 (1995).

[2] M. Liu, R. D. Farrant, J. K. Nicholson, and J. C. Lindon, J. Magn. Reson. Series A **112**, 208 (1995).

[3] M. Liu, R. D. Farrant, B. C. Sweatman, J. K. Nicholson, and J. C. Lindon, J. Magn. Reson. Series A **113**, 251 (1995).

[4] M. Liu, R. D. Farrant, J. K. Nicholson, and J. C. Lindon, Magn. Reson. Chem. **33**, 212 (1995).

[5] M. Liu, J. K. Nicholson, J. C. Lindon, P. N. Sanderson, and G. E. Tranter, Magn. Reson. Chem. **34**, 865 (1996).

[6] M. Liu, X. A. Moa, C. H. Ye, J. K. Nicholson, and J. C. Lindon, J. Magn. Reson. **129**, 67 (1997).

[7] M. Liu, R. D. Farrant, J. K. Nicholson, and J. C. Lindon, Mol. Phys. **99**, 1701 (2001).

[8] D. M. Doddrell, D. T. Pegg, and M. R. Bendall, J. Magn. Reson. **48**, 323 (1982).

[9] H. Bildsøe, S. Dønstrup, H. J. Jakobsen, and O. W. Sørensen, J. Magn. Reson. **53**, 154 (1983).

[10] M. Liu and J. C. Lindon, Curr. Org. Chem. **5**, 351 (2001).

[11] K. H. Gardner and L. H. Kay, Annu. Rev. Biophys. Biomol. Struct. **27**, 357 (1998).

[12] O. W. Sørensen, G. W. Eich, M. H. Levitt, G. Bodenhausen, and R. R. Ernst, Prog. NMR Spectrosc. **16**, 163 (1983).

[13] F. J. M. Van De Ven and W. C. Hilbers, J. Magn. Reson. **54**, 512 (1983).

[14] K. J. Packer and K. M. Wright, Mol. Phys. **50**, 797 (1983).

[15] J. Shriver, Concepts Magn. Reson. **4**, 1 (1992).

[16] N. Chandrakumar and S. Subramanian, Modern Techniques in High Resolution FT NMR, Springer, New York, USA 1987.

[17] N. Chandrakumar, J. Magn. Reson. **60**, 28 (1984).

[18] R. R. Ernst, G. Bodenhausen, and A. Wokaun, Principles of Nuclear Magnetic Resonance in One and Two Dimensions, Clarendon Press, Oxford 1987.

[19] A. Gençten and F. Köksal, Spectrosc. Lett. **30**, 71 (1997).

[20] A. Gençten and Ö. Tezel, Spectrosc. Lett. **34**, 317 (2001).

- [21] N. Chandrakumar, Spin-1 NMR, Springer, Berlin 1996.
- [22] P. J. Hore, J. A. Jones, and S. Wimperis, NMR: The Toolkit, Oxford University Press, New York 2000.
- [23] A. Gençten, Ö. Tezel, and A. Köroğlu, Appl. Magn. Reson. **20**, 265 (2001).
- [24] T. T. Nakashima, R. E. D. McClung, and B. K. John, J. Magn. Reson. **58**, 27 (1984).
- [25] T. Özdoğan, A. Gençten, and F. Köksal, Balkan Phys. Lett. **6**, 41 (1998).
- [26] A. Gençten, T. Özdoğan, and F. Köksal, Spectrosc. Lett. **31**, 981 (1998).
- [27] İ. Şaka and A. Gençten, Z. Naturforsch. **62a**, 259 (2007).
- [28] İ. Şaka and A. Gençten, J. Mol. Struct. **834**, 521 (2007).
- [29] A. Gençten, Ö. Tezel, and S. Bahçeli, Chem. Phys. Lett. **351**, 109 (2002).
- [30] İ. Şaka, Ö. Tezel, and A. Gençten, Z. Naturforsch. **58a**, 139 (2003).
- [31] Ö. Tezel, A. Gençten, A. Tokatlı, M. Şahin, and S. Bahçeli, Acta Phys. Pol. A **104**, 503 (2003).
- [32] A. Tokatlı, A. Gençten, M. Şahin, Ö. Tezel, and S. Bahçeli, J. Magn. Reson. **169**, 68 (2004).
- [33] N. Chandrakumar, H.-E. Mons, D. Hüls, and H. Günther, Magn. Reson. Chem. **34**, 715 (1996).
- [34] S. Venkata Raman and N. Chandrakumar, Mol. Phys. **90**, 855 (1997).
- [35] P. Allard and T. Härd, J. Magn. Reson. **153**, 15 (2001).
- [36] A. Gençten and İ. Şaka, Mol. Phys. **104**, 2983 (2006).
- [37] R. P. F. Kanters, B. W. Char, and A. W. Addison, J. Magn. Reson. Series A **101**, 23 (1993).
- [38] http://oncampus.richmond.edu/~rkanters/POF/